

Proteotronics: Application to Human 17-40 and Bacteriorhodopsin Receptors

Eleonora Alfinito¹, Lino Reggiani², Rosella Cataldo², Giorgio De Nunzio²,
Maria Rachele Guascito³ and Livia Giotta³

¹Dipartimento di Ingegneria dell'Innovazione, Università del Salento, via Monteroni, Lecce, Italy

²Dipartimento di Matematica e Fisica "Ennio de Giorgi", Università del Salento, via Monteroni, Lecce, Italy

³Dipartimento Di.S.Te.B.A., Università del Salento, via Monteroni, Lecce, Italy

Keywords: Protein Electrical Properties, Proteotronics.

Abstract: Human olfactory 17-40 and Bacteriorhodopsin are two protein receptors that received particular attention in electronics, due to the possibility of implementing nano-biodevices able to detect odours and light and thus useful for medical and green energy harvesting applications. Some recent experiments concerning the electrical responses of these receptors are reviewed. Data are interpreted in the framework of a new science exploiting the complexity in biology and biomedical engineering called proteotronics. In particular, the single protein is modelled as an impedance network whose topological properties affect the electrical response as measured by experiments.

1 FOREWORD

Recent advances in science and technology, such as the development of techniques and devices for health care and green and renewable energy, are the successful products of the synergy among different bailiwicks. As a matter of fact, cross-fertilization has diffused a consolidated knowledge beyond the boundaries of specific cliques, thus allowing the birth of a more comprehensive methodological approach which integrates and makes more powerful chemical, computational, biological, engineering and physical strategies (Alfinito, 2015a; De Nunzio, 2015; Guascito, 2011; Nagy, 2013).

Complexis 2016, being the first international conference on complex information systems, offers the relevant opportunity to introduce *proteotronics*, a new emerging discipline aiming to propose and develop innovative electronic devices, based on the selective action of specific proteins. The word originates from the combination of *proteomics*, the science devoted to the large-scale study of proteins structures and functions, and *electronics*, the science devoted to the development of devices manipulating electrical current to perform useful tasks.

2 INTRODUCTION

Proteins are the core of the cellular functions. They are macro-assemblies of hundreds to thousands of amino acids. Amino acids are taken by a set of about 20 elements and are structurally similar molecules, which differ for the specific R-group. Proteins carry out very different functions: they produce energy, transform chemicals, build tissues, etc. Their function is intimately connected to structure (Berg, 2002), which, in most cases, changes (conformational change) when the protein performs its activity. Therefore, a growing interest is devoted to determine protein 3D structures in the different phases of the protein activity. At present, the number of classified structures of proteins in their native state is quite large, while the structures of activated proteins are quite a few. As a matter of fact, the determination of the structure of proteins in their active state is much more complex than in their native state. This because structure and function are strongly connected and the measurement of the former may change the latter (Shrödinger, 1944). Protein activation itself is a big challenge of investigation, involving the mechanisms of internal binding rearrangements (Kobilka, 2007) and the modification of the protein free-energy landscape (Alfinito, 2015b). These and other questions have been recently investigated on a special family of

proteins, the receptors, i.e. proteins able to capture an external ligand (small proteins, molecules, light, etc.), then converting this capture into a biochemical signal. Recently, proteins have gained a primary role in advancing electronics performances toward a more friendly, green and renewable guise. The cornerstone of this interest is the possibility to equip electrical devices with the peculiar abilities of these proteins in recognizing, selecting and capturing specific ligand. These biochemical activities have a natural portability to the electronic world since they can be converted into electrical signals (Hou, 2007; Benilova, 2008; Vidic, 2006; Jin, 2006; Ron, 2010; Casuso, 2007). To take on this challenge it is necessary to gain knowledge about the protein features *in vivo* and *in vitro*, to achieve the experience for producing electronic nanodevices, to develop the ability for integrating organic and inorganic components, to collect information sufficient for producing a model of the physico-chemical mechanisms underlying the device response. The body of these studies has been recently named proteotronics (Alfinito, 2015a), by combining proteomics, the large-scale study of proteins, and electronics. In particular, we already showed some breaking results in protein electrical measurements and the way these results are interpreted into the framework of proteotronics. This is carried out by representing the protein like a complex network able to mimic the electrical responses observed in experiments and to be predictive for novel results.

In this paper we present the application of proteotronics for two receptors, the human olfactory receptor OR 17-40 and the bacteriorhodopsin. They received wide experimental investigation for their electrical properties as biological transducers when used as active parts of electronic devices. We selected those two cases as the best representative among the experimental datasets on which the theoretical model, drawn in the next section, has been validated. The content is organized as follows: Section 3 reports experimental and theoretical results concerning the electrical responses of human olfactory receptor OR 17-40, of high interest for the realization of bioelectronic noses. Section 4 reports experimental and theoretical results concerning the light receptor bacteriorhodopsin, of great interest for future applications in the field of green energy production; finally, Section 5 sketches the main conclusions.

3 HUMAN OR 17-40

3.1 Generalities and Experiments

Recent investigations have confirmed the possibility of detecting the protein activity by using electrical measurements (Vidic, 2006; Jin, 2006; Hou, 2007; Benilova, 2008; Guascito, 2011; Nagy, 2014). All the analyzed proteins (mainly olfactory and light receptors) show a characteristic impedance response, which strongly depends on the protein structure and on the environmental conditions. In other terms, measurements of the electrical responses are a sensitive tool for detecting protein conformational change (activation). The present case concerns the activation of human olfactory receptor OR 17-40. This protein shows a very good sensitivity to helional and heptanal odorants (Levasseur, 2003; Vidic, 2006; Benilova, 2008), although the results deviate from a standard expectation and need for a microscopic interpretation (Alfinito, 2011b).

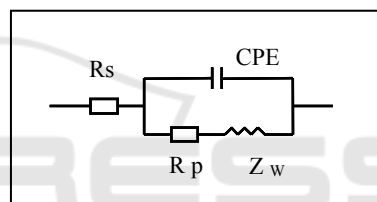


Figure 1: Randles cell. R_s is the solution resistance and R_p , Z_w and CPE, the polarization resistance, the Warburg impedance, and the constant phase element of the sample, respectively.

Here we report experiments performed by using the electrochemical impedance spectroscopy (EIS) (Benilova, 2008).

The experimental set-up involves protein receptors in their membrane fraction, anchored on properly functionalized specific substrates and used to detect the *in vitro* dose- response to their specific ligands. In particular, EIS measurements were performed under different concentrations of the protein specific odorants and for each concentration an impedance spectrum was recorded. The standard procedure to interpret the impedance spectrum is to give a simplified representation of the apparatus by using a Randles cell, like that shown in Figure 1. In particular, R_p is the element more sensitive to the protein activation. Therefore, measurements of its value with and without the odorant were performed.

At increasing values of the specific odorant concentration, the polarization resistance shows a peculiar bell-shaped behavior, centered at 10^{-10} M (Benilova, 2008). Furthermore, by using

complementary techniques such as the differential surface plasmon resonance (SPR) and the differential bioluminescence response, also a second peak was observed, at a higher concentration of the odorant (around 10^{-5} M) (Vidic, 2006). This kind of response, that does not exhibit a saturation at the highest concentrations, is unexpected.

3.2 Theory

The protein structure-function correlation is here interpreted at the amino acid level, building a graph whose nodes correspond to the amino acids. Each node contains several data, like the amino acid position, taken by the public data banks (Berman, 2002), and its electrical polarization in terms of a specific dielectric constant (Alfinito, 2011a). These data are used to assign the links between nodes that are associated with an elemental impedance responsible of charge transfer. The procedure to construct the analogous network of the protein requires two steps. In the first step, an interaction radius, R_C , is assigned. It determines the degree of the graph nodes, because two nodes are connected only if the physical distance between the corresponding amino acids is less than R_C (Figure 2).



Figure 2: Graphical representation of human OR 17-40 in its native state. The network is obtained by using $R_C = 6 \text{ \AA}$.

Furthermore, this kind of network preserves the memory of the protein structure, i.e. it changes if the protein 3D structure changes. In the second step, the protein function is then introduced, by attributing to the links the role of a specific physical interaction. In the present case, it is an electromagnetic interaction, that describes the response of the protein to different electrical solicitations, thus the links correspond to elementary impedances. In particular, since we are interested in monitoring the impedance

variation due to the protein activation, we use the impedance of a simple RC parallel circuit, like the couple CPE-Rp in the Randles cell.

Finally, the elemental impedance between the i,j -th nodes is:

$$Z_{i,j} = \frac{l_{i,j}}{A_{i,j}} \frac{1}{\rho^{-1} + i\epsilon_{i,j}\epsilon_0\omega} \quad (1)$$

where $A_{i,j} = \pi(R_C^2 - l_{i,j}^2/4)$, is the cross-sectional area between two spheres of radius R_C centered on the i -th and j -th node, respectively; $l_{i,j}$ is the distance between these centers, ρ is the resistivity, taken to be the same for every amino-acid; $i = \sqrt{-1}$ is the imaginary unit, ϵ_0 is the vacuum permittivity, ω is the circular frequency of the applied voltage. The relative dielectric constant of the couple of i -th and j -th amino-acids, $\epsilon_{i,j}$, is expressed in terms of the intrinsic polarizability of each amino acid. The network is connected to an external bias by using ideal contact on the first and last amino acid and solved by using standard techniques. In particular, analogously to the well known Hodgkin-Huxley model, the problem statement consists in a set of linear equations whose solution is performed by a computational procedure, based on the Kirchhoff's laws. The network global impedance spectrum is represented by a Nyquist plot for each configuration of the protein 3D structure. The role of the interaction radius, R_C , is still an open problem. Recent investigations strongly suggest that it is related to the level of protein activation (Kobilka, 2007; Alfinito, 2015b) and in the following section we make use of this conjecture to interpret the experiments.

Besides the electrical characterization, also a preliminary description in terms of graph topology was attempted. The molecule networks resulting from setting the interaction radius to reasonable values were found to be graphs with a small-world structure (Albert, 2002). Small-world networks emerge as intermediate configurations between the limiting cases of regular lattices and completely random graphs. Artificial generation of a small-world network can be obtained by the Watts-Strogatz model, in which a fraction p of the links of a regular lattice is replaced with random links: of course p is 0 for the regular lattice, and becomes 1 for a completely random network. In small-world networks the distribution of node degrees is Poisson-like, and the Average Path Length is short, like in random networks, but the Clustering Coefficient is quite high, like in regular lattices.

3.3 Results

As a preliminary test, we analyze the relative variation of static impedance (resistance) for the single protein in the presence/absence of the ligand. Globally small differences are detectable and, in agreement with experiments only two regions of R_C values centred around 20 and 50 Å are of interest, because the native state resistance exhibits a higher value than the active state (Benilova, 2008). In agreement with (Kobilka, 2007) we have postulated a functional dependence of the odorant concentration on the value of R_C (Alfinito, 2011b).

In Figure 3 we report the relative resistance variations, calculated with our model. Furthermore, symbols describe the same quantity as observed in experiments performed with helional and heptanal.

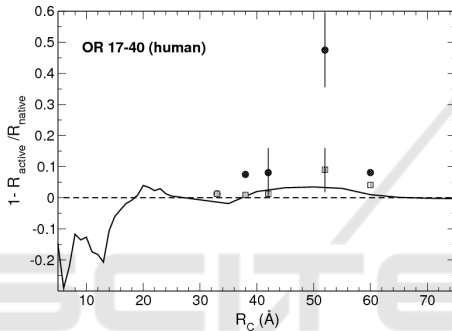


Figure 3: Relative resistance variation for human olfactory receptor OR 17-40. Continuous line is the calculated result, full circles (empty squares) are the dose response to heptanal (helional) by experimental data (Benilova, 2008), here given in terms of R_C (Alfinito, 2011a).

The bump at lower value of R_C , should be, in a similar way, attributed to the second bump observed by SPR. As we can see, the agreement is qualitative and more close to the heptanal than to the helional data.

Further improvement of the model are necessary to quantitatively fit experimental outcomes (Alfinito, 2015b).

These results are confirmed by the analysis of the impedance spectrum. The Nyquist plots, as calculated by using the native and active state of OR 17-40 are reported in Figure 4. Continuous line describes the receptor impedance spectrum in the native state calculated by using $R_C = 50$ Å and the dashed line to the active state with the same value of R_C . As a comparison, data obtained with protein exposed to a concentration of 10^{-10} M of heptanal, normalized to the static impedance of the protein not exposed to the odorant are also reported (dots) (Alfinito, 2011b). The agreement is qualitatively

correct, i.e. the spectrum is represented by a simple semicircle and the shrinking of the semicircle, when going to the activated state, is also reproduced. As a general outcome, the comparison between theory and experiment is quite good and able to explain the quite novel results concerning the protein response to the specific ligands.

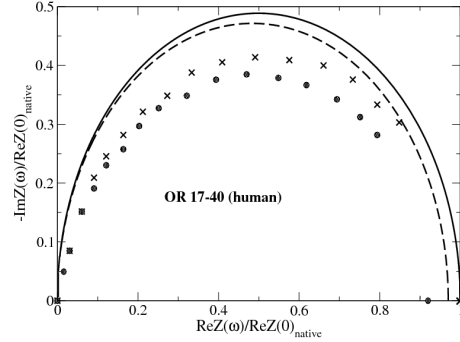


Figure 4: Normalized Nyquist plot of human OR 17-40. Lines (continuous for native state, dashed for active state) refer to calculated data, with $R_C = 50$ Å. Dots refer to experimental data for the protein with heptanal at a concentration of 10^{-10} M, crosses to the protein without heptanal (Benilova, 2008).

Finally, concerning the small-world features of the network, the node degree distribution was calculated, giving a bell-shaped curve. The calculation was done at two values of the interaction radius, $R_C = 6$ Å and $R_C = 12$ Å, and the behaviour of the frequency curve in the transition from the smaller to the larger R_C value was as expected, i.e. the bell width increases while its mean value gets larger like in the Poisson distribution, which is considered a good approximation for random networks (Figure 5).

The average path length L and the clusterization coefficient C were also calculated, together with the same values normalized to C_R and L_R (which are the clusterization coefficient and the average path length calculated for a regular lattice with equal number of nodes N and equal mean degree, MD). The result was a large C (far greater than $O(N^{-1})$ which would be typical of random graphs, and similar to C_R) and a relatively low average path length, which is compatible with the hypothesis of a small-world network with significant clusterization. This is particularly true for the lower R_C case (see Table 1).

Table 1: Network parameters for human OR 17-40.

N	R_C (Å)	MD	C	C/C_R	L	L/L_R
315	6	6.1	0.56	0.93	8.3	0.31
315	12	29.5	0.59	0.81	3.0	0.53

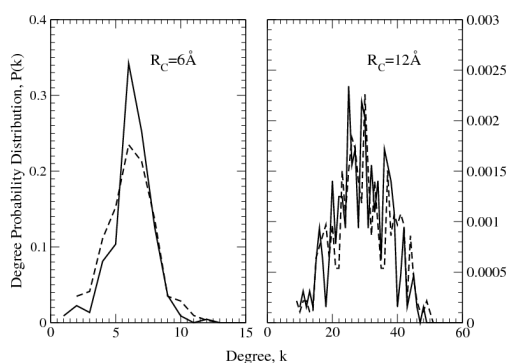


Figure 5: Degree distribution of human OR 17-40 (dashed lines) and bacteriorhodopsin (continuous lines), obtained by using $R_c = 6 \text{ \AA}$ and $R_c = 12 \text{ \AA}$.

4 BACTERIORHODOPSIN

4.1 Generalities and Experiments

Another receptor of interest for applications is bacteriorhodopsin (bR), a protein found in a primeval organism, the *Halobacterium salinarum*, specifically in a part of its cell membrane called the purple membrane (PM). This membrane is a very thin lipidic film of 5 nm, about the protein height, and shows a quite stable structure.

Bacteriorhodopsin is able to convert the sun light into an electrical potential across the host cell membrane. In doing so, the conjugated dye, the retinal, changes its structure, also inducing the complete protein conformational change.

Recently, several experiment have analyzed bR, *in vitro*, both in dark and light. The aim was to test the possibility of recovering the activity of this protein outside its natural environment and finally to convert the activation due to light into an electrical signal useful for technological applications.

In doing so, patches of PM were anchored on a conductive substrate and connected to an external circuit. The connection was made mainly with two different techniques, i.e, by using an extended transparent conductive contact (Jin 2006, Ron 2010) or the tip of a c-AFM (Casuso, 2007; Mukhopadhyay, 2014).

These investigations focused on the measurement of the current-voltage (I-V) characteristics in static conditions and revealed the great stability of bacteriorhodopsin toward thermal, mechanical and electrical stress (Casuso, 2007). This protein shows a medium-gap conductivity in dark which can be significantly enhanced by light. The

observed I-V characteristics are super-linear, and this feature becomes more evident by increasing the applied bias. Therefore, the charge transport across the protein is mainly attributed to a tunneling mechanism. Tunneling can be described like the crossing of rectangular barriers at low bias (direct tunneling), or the crossing of triangular barriers (injection tunneling), at high bias. In the latter regime, a growth of the protein current of about 5 orders of magnitude has been observed (Casuso, 2007). All these impressive features require a deep investigation about the microscopic origin of the responsible mechanisms. Furthermore, they have arisen great expectations in technology, so inspiring, for example, the realization of a Grätzel cell based on it (Renugopalakrishnan, 2014).

It has been observed that the light protein activation may produce an enhancement of the current as large as the 100% (Jin, 2006). In the perspective of a future use of this protein in solar cell, this outcome is of extraordinary relevance.

4.2 Theory

The network protein analogue has been also used to describe the observed I-V characteristics in bR and other proteins (Alfinito, 2015a). In Figure 6, the plot of the protein graph, drawn by using $R_c = 6 \text{ \AA}$, is reported. As a matter of fact, light induces a conformational change that this model is able to account for. Accordingly, a sequential tunneling mechanism is introduced by using a stochastic approach within a Monte Carlo solving technique.

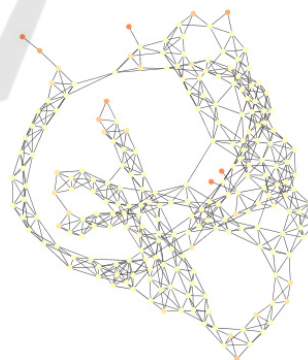


Figure 6: Graphical representation of bacteriorhodopsin in its native state. Network is obtained by using $R_c = 6 \text{ \AA}$.

The non-linear shape of the I-V characteristic, reported in (Jin, 2006; Casuso, 2007), is accounted for by considering a tunneling probability including direct and injection regimes, respectively, as in (Alfinito, 2011a; Alfinito, 2014):

$$\begin{aligned}
 P^{DT}_{ij} &= \exp\left(-\beta\sqrt{\Phi - \frac{eV_{ij}}{2}}\right), & eV_{ij} < \Phi \\
 P^{IN}_{ij} &= \exp\left(-\beta\frac{\Phi}{eV_{ij}}\sqrt{\frac{\Phi}{2}}\right), & eV_{ij} \geq \Phi
 \end{aligned} \quad (2)$$

where V_{ij} is the potential drop between the couple of i-j amino acids, $\beta = \left(2l_{ij}\sqrt{2m}\right)/\hbar$, m the electron effective mass. In this model, to tunnel an energy barrier is equivalent to reduce the resistivity from its maximum value down to $\rho_T(V)$:

$$\rho_T(V) = \rho_{\min} \quad (3a)$$

in direct tunneling regime (rectangular barrier), and:

$$\begin{aligned}
 \rho(V) &= \rho_{\max}, & eV < \Phi \\
 \rho(V) &= \rho_{\max} \frac{\Phi}{eV} + \rho_{\min} \left(1 - \frac{\Phi}{eV}\right), & eV \geq \Phi
 \end{aligned} \quad (3b)$$

in the injection tunneling regime (triangular barrier).

4.3 Results

The I-V characteristics of bR in dark and light have been calculated by using the aforementioned theoretical approach. In particular, the model parameters have been tuned on the data given by (Casuso, 2007), which cover the largest bias range.

In such a way, the experiments have been reproduced with good accuracy (Alfinito, 2011a). Data in light were given by (Jin, 2006) in the range 0-1 V. A fine agreement with these data has been found by taking into account the multiple effects that light produces on a sample of light receptors. In particular, light irradiation transfers energy to the single protein by means of two basic processes: (i) the protein activation, specifically the change of its 3D structure consequent the ligand capture; and (ii) the protein excitation, specifically the increasing of its free-energy without conformational change (Alfinito, 2015).

In the framework of our model, we introduce process (i) by changing the 3D protein structure input, while process (ii) is described by changing the value of R_C . Finally a sample of proteins irradiated with light of appropriate wavelength experiences both the processes, with some proteins activated and some proteins excited. The percentage of activated/excited proteins has been fitted by using a Hill-like equation, and it is associated with a specific value of R_C (Alfinito, 2015). Therefore, following

this scheme, the current response of bR samples has been reproduced by using a binary mixture of native and active states:

(i) the sample in light corresponds to $R_C = 6.3 \text{ \AA}$ with 96% of activated proteins, (ii) the sample in dark corresponds to $R_C = 5.8 \text{ \AA}$ and 100% of proteins in the native state. By using these guidelines, we reproduce the photocurrent measured in experiments. Figure 7 reports the photocurrent of bR calculated within our model, in the same bias range explored by (Casuso, 2007).

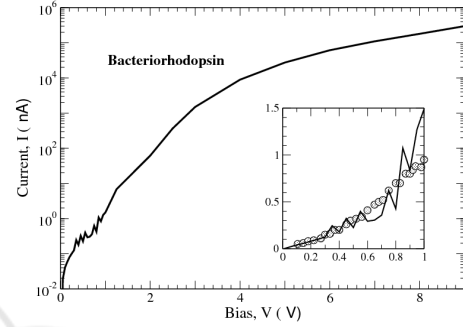


Figure 7: Photocurrent for the bacteriorhodopsin, calculated as described in the text. In the inset, the same data in the bias range 0-1 V and the experimental outcomes (circles) (Jin, 2006).

Furthermore, the theoretical approach is able to foresee photocurrent over a larger (*a priori*, arbitrary large) bias range. At present only the bias range described in the inset has been explored by experiments (Jin, 2006).

Also for this protein we checked the network small-world character. The node degree distribution was again bell-shaped (not shown for the sake of brevity) and very similar to what was found for OR 17-40 (see Fig.5). The (absolute and relative) average path length and clusterization coefficient are shown in Table 2.

Table 2: Network parameters for bacteriorhodopsin.

N	R_C (Å)	MD	C	C/C_R	L	L/L_R
222	6	6.2	0.58	0.96	7.0	0.37
222	12	28.9	0.59	0.82	2.6	0.60

Again, the lower R_C case is more easily framed in a small-world context, having large C/C_R and low L/L_R .

5 CONCLUSIONS

Proteotronics is an emergent branch of electronics,

able to describe the electrical properties of proteins. The model is physically plausible and sufficiently flexible to be tailored for describing different experimental conditions. Here we have investigated two specific cases concerning human OR 17-40 and bacteriorhodopsin protein receptors with promising chances of being used in developing a new generation of electronic devices. The results are also of basic interest in advancing the present knowledge on the microscopic mechanisms responsible of protein functioning inside living cells.

REFERENCES

- Albert, R. and Barabási, A.L. 2002. Statistical mechanics of complex networks. *Reviews of modern physics*, 74(1), p.47.
- Alfinito, E., Millithaler, J-F. and Reggiani, L. 2011. Charge transport in purple membrane monolayers.... *Physical Review E* 83, no. 4 pp. 042902.
- Alfinito, E., Millithaler, J.F., Reggiani, L., et al. 2011. Human olfactory receptor 17-40 *RSC Advances*, 1(1), pp.123-127.
- Alfinito, E. and Reggiani, L. 2014 Opsin vs opsin: New materials for biotechnological applications. *Journal of Applied Physics* 116 (6), p. 064901.
- Alfinito, E., Pousset, J-F., and Reggiani, L. 2015. *Proteotronics: Development of Protein-Based Electronics*, Pan Stanford, Singapore.
- Alfinito, E. and Reggiani, L. 2015. Mechanisms responsible for the photocurrent in bacteriorhodopsin. *Physical Review E*, 91(3), p.032702.
- Benilova, I.V., Vidic, J.M., Pajot-Augy, et al. 2008. Electrochemical study of human olfactory receptor OR 17-40.... *Materials Science and Engineering: C*, 28(5), pp.633-639.
- Berg, J.M., Tymoczko, J.L., Stryer, L. 2002 *Biochemistry*, W H Freeman, New York, V edition.
- Berman, H.M., Westbrook, J., Feng, Z., et al. 2000. The protein data bank. *Nucleic acids research*, 28(1), pp.235-242.
- Casuso, I., Fumagalli, L., Samitier, J., et al. 2007. Nanoscale electrical conductivity of the purple membrane monolayer. *Physical Review E* vol 76(4), pp. 04191.
- De Nunzio, G., Cataldo, R. and Carlà, A. 2015. Robust Intensity Standardization *Journal of digital imaging*, pp.1-11.
- Guascito, M.R., Chirizzi, D., Malitesta, C. et al. 2011. Mediator-free amperometric glucose biosensor *Analyst*, 136(1), pp.164-173.
- Hou, Y., Jaffrezic-Renault, N., Martelet, et al. 2007. A novel detection strategy for odorant molecules... *Biosensors and Bioelectronics*, 22(7), pp.1550-1555.
- Jin, Y., Friedman, N., Sheves, M., He, T. and Cahen, D. 2006. Bacteriorhodopsin (bR) as an electronic conduction medium: Current transport through bR-containing monolayers. *Proceedings of the National Academy of Sciences*, 103(23), pp.8601-8606.
- Kobilka, B.K. and Deupi, X. 2007. Conformational complexity of G-protein-coupled receptors. *Trends in pharmacological sciences*, 28(8), pp.397-406.
- Levasseur, G., Persuy, M.A., Grebert, D., et al. 2003. Ligand-specific dose-response.... *European Journal of Biochemistry*, 270(13), pp.2905-2912.
- Nagy, L., Magyar, M., Szabo, T., et al. 2013. Photosynthetic Machineries in Nano-Systems. *Current Proteins and Peptide Science*, 15 pp.363-373
- Renugopalakrishnan, V., Barbiellini, B., King, C., et al. 2014. Engineering a Robust Photovoltaic Device with Quantum Dots and Bacteriorhodopsin. *J. Phys. Chem. C*, 118, pp.16710-16717
- Ron, I., Sepunaru, L., Itzhakov, S., et al 2010. Proteins as electronic materials...*Journal of the American Chemical Society*, 132(12), pp.4131-4140.
- Shrödinger, E. 1944 *What is life?* Cambridge University, Cambridge.
- Vidic, J.M., Grosclaude, J., Persuy, M.A., et al. 2006. Quantitative assessment of olfactory receptors activity... *Lab on a Chip*, 6(8), pp.1026-1032.